O-B9

Surface reactive micro/nano particles on inorganic oxygen separation membrane

Kee Sung Lee, Tae Ho Shin*, Shiwoo Lee*, Sang Kuk Woo**,
Jae Kyo Yang** and Yong Ho Choa**
School of Mechanical & Automotive engineering, Kookmin University, Seoul, 136-702, Korea,
*Korea Institute of Energy Research, Daejeon, 305-343, Korea,
**Dept. of Chemical Eng., Hanyang University, Ansan, 425-791, Korea

Tel. +82 (02) 910-4834 ; Fax. +82 (02) 910-4839 ; email: keeslee@kookmin.ac.kr

Abstract

Micro/nano-sized $La_{0.6}Sr_{0.4}CoO_{3-\delta}$ particles are considered to improve oxygen permeability in highly selective inorganic oxygen separation membrane. A $La_{0.7}Sr_{0.3}Ga_{0.6}Fe_{0.4}O_{3-\delta}$ membrane with perovskite structure is fabricated by a conventional solid-state reaction. As the oxygen permeation flux of the $La_{0.7}Sr_{0.3}Ga_{0.6}Fe_{0.4}O_{3-\delta}$ membrane was lower than commercial gas separation membranes, we coated the $La_{0.6}Sr_{0.4}CoO_{3-\delta}$ particles to enhance the oxygen permeation flux. It has been demonstrated that the effective area of reactive free surface is an important factor in determining the effectiveness of the introduction of coating layer for oxygen permeation. The introduction of micro/nano $La_{0.6}Sr_{0.4}CoO_{3-\delta}$ particles was very effective for increasing oxygen flux, as the flux was as much as 2 to 6 times higher than that of an uncoated $La_{0.7}Sr_{0.3}Ga_{0.6}Fe_{0.4}O_{3-\delta}$ membrane.

Key Words : $La_{0.7}Sr_{0.3}Ga_{0.6}Fe_{0.4}O_{3-\delta}$; $La_{0.6}Sr_{0.4}CoO_{3-\delta}$ coating; Perovskite; Membrane reactor; Oxygen permeation;

1. Introduction

Dense Inorganic membranes are used for water purification, particle separation, and gas separation because of higher temperature resistance and superior corrosion resistance over metals or polymer-based membranes [1]. While most inorganic membranes include pores to select a particular element, dense membranes are used as a gas separation membrane [1]. An oxygen permeable dense ionic conductor has been drawing considerable attention recently because of its spontaneous oxygen mobility under an oxygen concentration gradient at high temperature as well as high selectivity [1,2]. This membrane is usually applicable for syngas production by partial oxidation of methane gas, oxygen-enriched fuel burner system and the electrode of solid oxide fuel cell. Membrane reactors have attracted increasing attention for the syngas production because they have advantage in simple design and energy saving process.

In theses membranes, oxygen transportation occurs spontaneously under the oxygen concentration gradient through oxygen vacancy in the lattice of membrane [3,4] at high temperatures of around 600°C ~ 1000°C. $LaCoO_3$ based ceramic membranes have been studied since Teraoka found that perovskite-typed membrane shows higher ionic conductivity than yttria stabilized zirconia [2]. To produce oxygen vacancy to facilitate mobility of oxygen, the other element, A′, is replaced in the A site of ABO_3. For example, Sr^{2+} ion substitution for La^{3+} ion site in $LaFeO_{3-\delta}$ perovskite oxide forms oxygen vacancies and causes a change of valence states in B-site cations so that charge neutrality is maintained. However, even though they have higher oxygen permeation flux, the membranes showed lower stability in severely reduced atmosphere, which results in phase transformation and microstructural change during long time operation [5-7]. Therefore, more recently, a composition, $La_{0.7}Sr_{0.3}Ga_{0.6}Fe_{0.4}O_{3-\delta}$, has been reported to have a good chemical, structural stability, but also to have limited oxygen permeability [8-9].

In the present study, we thus evaluated the effect of surface modification by $LaSrCoO_3$ onto $LaSrCoFeO_3$ and $LaSrGaFeO_3$ by presenting

data on their fundamental oxygen permeating properties at elevated temperature. We also discuss the decisive factors in determining the surface exchange kinetics of the $LaSrCoO_3$ coating layer. All through the paper, $La_{0.6}Sr_{0.4}Co_{0.2}Fe_{0.8}O_{3-\delta}$ oxide is designated by the abbreviation LSCF. Similarly, $La_{0.7}Sr_{0.3}Ga_{0.6}Fe_{0.4}O_{3-\delta}$ and $La_{0.6}Sr_{0.4}CoO_{3-\delta}$ compositions are designated as LSGF and LSC respectively.

2. Experimental Procedure

Perovskite membranes, LSCF and LSGF, were fabricated using a conventional solid-state reaction method. Precise amounts of La_2O_3 (99.999%, Aldrich Chemical Co.; the rest are the same), $SrCO_3$ (99.9%), Fe_2O_3 (99%), and $Co(NO_3)_2 \cdot 6H_2O$ (98%) or Ga_2O_3 (99.99%) powders were mixed in isopropyl alcohol with a ZrO_2 ball for 24h. The starting compositions were controlled to produce final molar ratio of La:Sr:Co:Fe=6:4:2:8 for LSCF and La:Sr:Ga:Fe=7:3:6:4 for LSGF. The powder mixture was calcined at 1000°C for 5 hrs for LSCF, and 1250°C for 5 hrs for LSGF. Calcined particles were uniaxially compressed into 1 inch (25.4 mm) diameter disks, followed by cold-isostatic pressing at 140 MPa. LSCF samples were sintered in air at 1300°C for 3 hrs and LSGF samples at 1500°C for 5 hrs. Both sides of the sintered membrane were ground and polished to 5 μm to give a final thickness of approximately 1.7 mm for permeation measurements. The micro-sized LSC particles were synthesized by mixing La_2O_3, $SrCO_3$, and $Co(NO_3)_2 \cdot 6H_2O$ and then calcined at 1000°C for 5 hrs. The particle mixtures were mixed into a paste with an organic solvent, binders, a plasticizer, and dispersant. Coating slurry was 60wt% of solvent with organic additives that were composed of 7wt% of ethyl cellulose for binder, 2wt% of fish oil for dispersant, 3wt% of polyethylene glycol for plasticizer, 3wt% of dibutylphthalates for the plasticizer, and 85wt% of solvent. The LSC particles were coated on both sides of the sintered membrane by a screen-printing method using 200 meshes screen. Post-heat treatment was conducted to remove the organic additives at 600°C for 5 hrs and to control the porosity of the coating layer at 800 ~ 1250°C for 2 hrs.

The gas-flow arrangement is schematically represented in Fig. 1, with specimen-reactor configurations. The membrane specimen, 19 mm diameter × 1.7 mm thick, was placed on the alumina tube with an Ag-ring as a gas-tight seal. To ensure sealing, the alumina tube and the specimen were fastened by a screwed alumina-cap. Helium (99.999%) was used as a sweeping gas and flushed over the surface of the membrane. The oxygen content of the permeate-stream was measured using gas chromatography (DS-6200, DONAM instrument), which used helium as a carrier gas. Measuring the nitrogen content in the permeate-stream checked for leakage of the feed gas through an incomplete Ag seal.

The nano-sized polycrystalline perovskite-type oxide LSC particles were prepared using a spray pyrolysis process. Each nitrides, $La(NO_3)_3$, $Sr(NO_3)_2$, and $Co(NO_3)_2 \cdot 6H_2O$ with molar composition La:Sr:Co = 6:4:10, were mixed with deionized water using a magnetic stirrer for 24hr. The precursor solution (0.1mol%) was converted to fine mist and passed through the hot zone of the furnace at a temperature of 1000°C to synthesize nano-sized particles. The synthesized particles were investigated using a TEM.

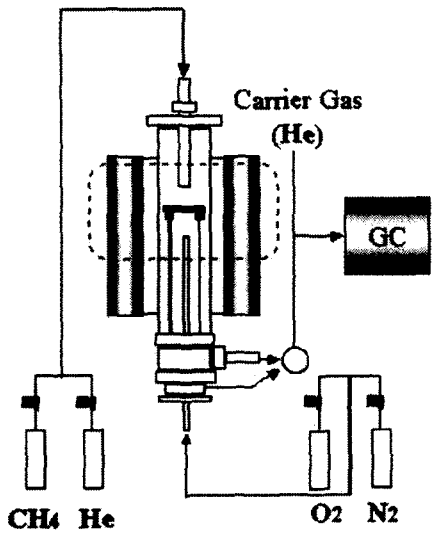

Fig. 1. Schematic diagram of gas-flow arrangement and oxygen permeability measuring system.

3.Results and discussion

Figure 2 shows the oxygen permeation fluxes as a function of operation temperature for LSCF and LSGF membrane. The flux was measured for the membrane without the introduction of LSC particles on the membrane surface. For the LSGF membrane, the oxygen was not permeated

until reaching at 900°C. On the other hand, oxygen started to permeate at around 800°C for LSCF membrane. It is notable that the oxygen flux of LSCF is as 2~3 times higher than LSGF at the highest temperature of this study, 950°C.

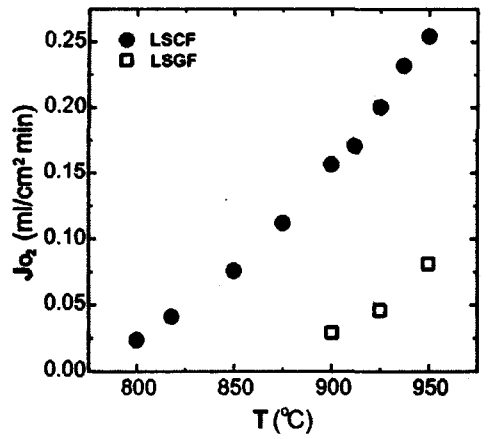

Fig. 2. Oxygen permeability of LSCF and LSGF as a function of temperature.

On the other hand, temperature dependencies of oxygen permeation flux with the introduction of LSC particles and the corresponding Arrhenius plot are shown in Fig. 3 and Fig. 4, respectively. While the oxygen permeated flux of uncoated LSGF membrane showed smaller value than that of LSCF, the porously LSC-coated LSGF (P-LSC/GF) significantly improved the oxygen permeability. On the other hand, there was no recognizable difference in the oxygen fluxes between LSCF and porously LSC-coated LSCF (P-LSC/CF) membrane. The results imply that the oxygen permeation kinetic of LSGF could be governed by the surface-exchange mechanism, while that of LSCF be only governed by a bulk diffusion process.

We compared three kinds of LSC layer configurations: (i) porous, (ii) dense, and (iii) outer-porous/inner-dense layers (abbreviated as PD-LSC/GF) in both surfaces of the LSGF membrane. The oxygen permeation fluxes of three kinds of surface-modified specimens are represented with that of unmodified LSGF as a function of reciprocal temperature in Fig. 5. The slope of the curve corresponds to the activation energy for oxygen permeation. Note the lower slope in P-LSC/GF at higher temperature. Although the activation energy of D-LSC/GF is lower than that of unmodified LSGF, it is not as low as P-LSC/GF at higher temperature region. The difference in the fluxes between D-LSC/GF and P-LSC/GF can be explained by the disparity in effective surface area. On the other hand, the flux of PD-LSC/GF was almost identical with that of P-LSC/GF over the entire temperature range measured. This result means that it is not the population of triple phase points but rather effective surface area that is the decisive factor in surface exchange reactivity of LSC.

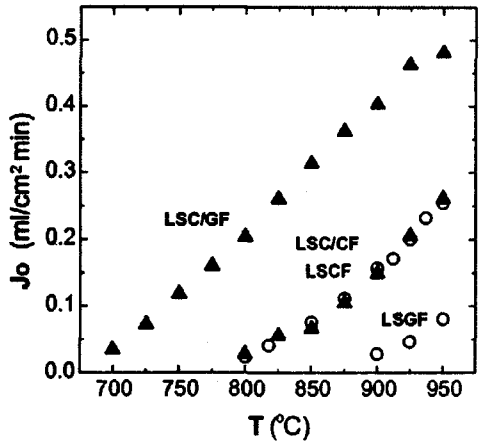

Fig. 3. Oxygen permeability of LSCF, LSGF, porous LSC-coated LSCF and porous LSC-coated LSGF as a function of temperature.

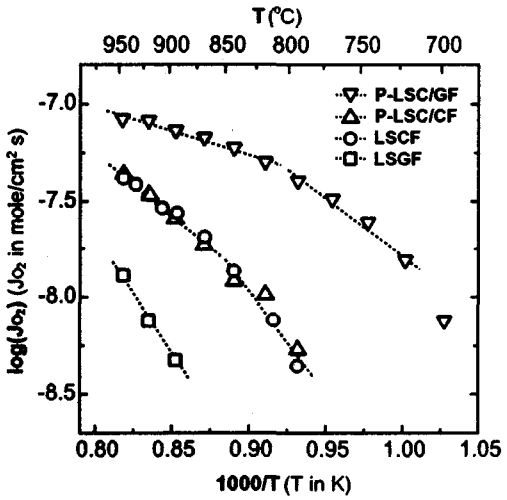

Fig. 4. Oxygen permeability of LSCF, LSGF, porous LSC-coated LSCF and porous LSC-coated LSGF as a function of reciprocal temperature.

TEM micrograph of representative LSC powder aggloermate prepared at 1000°C, solution concentration of 0.1 mol%, is shown in Fig. 6. It can be observed that spherical particles are the dominant morphology. The important characteristic of the powders obtained by our spray pyrolysis process was that the hollow (porous) particles could be obtained with highly inner surface area. It is expected that the increased

particles may contribute to the improvement of oxygen permeability more if it is well controlled during heat treatment process.

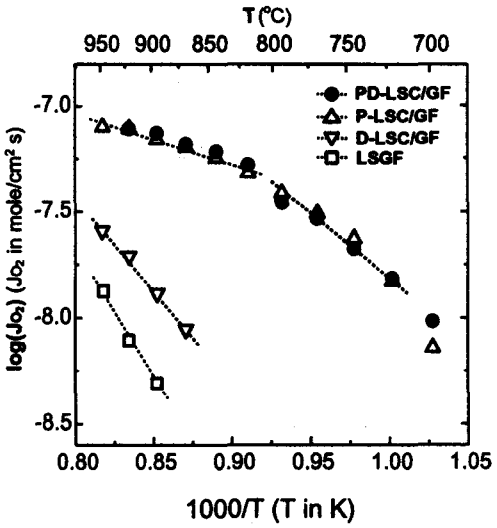

Fig. 5. Arrhenius plots of oxygen permeation fluxes of porous LSC-coated LSGF (P-LSC/GF), dense LSC-coated LSGF (D-LSC/GF) and outer-porous/inner-dense LSC-coated LSGF (PD-LSC/GF). For comparison, the oxygen permeation flux of uncoated LSGF (LSGF) is also represented.

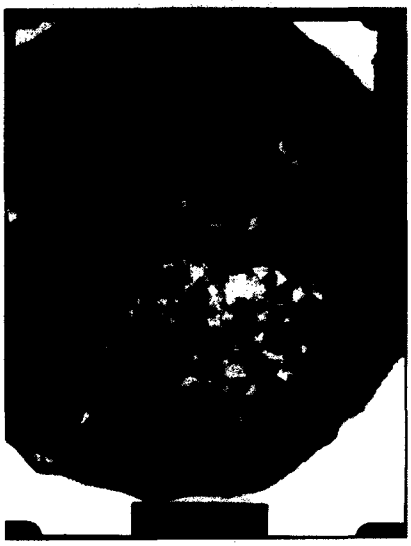

Fig. 6. TEM micrograph of LSC nanopowders synthesized from a 0.1 mol% solution, at 1000°C, using spray pyrolysis process (bar scale = 50nm).

4. Conclusions

Surface reactive micro-sized particles, $La_{0.6}Sr_{0.4}CoO_{3-\delta}$, was introduced for $La_{0.6}Sr_{0.4}Co_{0.2}Fe_{0.8}O_{3-\delta}$ and $La_{0.7}Sr_{0.3}Ga_{0.6}Fe_{0.4}O_{3-\delta}$ perovskite-typed oxygen permeation ceramic membrane. A significant improvement in the oxygen fluxes was obtained by introducing a highly surface exchange-reactive coating layer on the $La_{0.7}Sr_{0.3}Ga_{0.6}Fe_{0.4}O_{3-\delta}$ membrane. In particular, the oxygen flux was strongly influenced by the effective surface area in controlling the surface-exchange reaction kinetics. Nano-sized $La_{0.6}Sr_{0.4}CoO_{3-\delta}$ particles were successfully synthesized for further improvement of oxygen permeability in the stable ceramic membrane with high oxygen selectivity.

References

1. A. J. Burggraff and L. Cot, Fundamentals of Inorganic Membrane Science and Technology, Elsevier, Amsterdam, 1996.
2. Y. Teraoka, H. M. Zhang, S. Furukawa and N. Yamazoe, Oxygen Permeation through Perovskite-type Oxides, Chem. Lett., (1985) 1743-46.
3. J. W. Stevenson, T. R. Armstrong, R. D. Carneim, L. R. Pederson, W. J. Weber, Electrochemical Properties of Mixed Conducting Perovskite $La_{1-x}M_xCo_{1-y}Fe_yO_{3-\delta}$ (M=Sr, Ba, Ca), J. Electrochem. Soc., 14 3 (1996) 2722-2729.
4. L. Shiguang, W. Jin, P. Huang, N. Xu, J. Shi and Y. S. Lin, Tubular Lanthanum Cobaltite Perovskite Type Membrane for Oxygen Permeation, J. Membr. Sci., 166 (2000) 51-61.
5. B. Ma, U. Balachandran, J. H. Park, C. U. Segre, Electrical Transport Properties and Defect Structure of $SrFeCo_{0.5}O_x$, J. Electrochem. Soc., 143 (1996) 1736-1744.
6. S. Kim, Y. L. Yang, R. Christoffersen, A. J. Jacobson, Oxygen Permeation, Electrical Conductivity and Stability of the Perovskite Oxide $La_{0.2}Sr_{0.8}Cu_{0.4}Co_{0.6}O_{3-x}$, Solid State Ionics, 104 (1997) 57-65.
7. Y. S. Lin and Y. Zeng, Catalytic Properties of Oxygen Semipermeable Perovskite-type Ceramic Membrane Materials for Oxidative Coupling of Methane, J. Catal., 164 (1996) 220-231.
8. T. Ishihara, T. Shibayama, M. Honda, H. Nishiguchi and Y. Takita, Intermediate Temperature Solid Oxide Fuel Cell Using $LaGaO_3$ Electrolyte, J. Electrochem. Soc., 147 (2000) 1332-1337.
9. Y. Tsuruta, T. Todaka, H. Nisiguchi and T. Ishihara, Mixed Electronic-Oxide Ionic Conductor of Fe-Doped La(Sr)GaO3 Perovskite Oxide for Oxygen Permeating Membrane, Electrochemical and Solid State Letters, 4 (2001) E13-E15.